Determination of Adsorption Isotherms of Overpotentially Deposited Hydrogen on Platinum and Iridium in KOH Aqueous Solution Using the Phase-Shift Method and Correlation Constants

Jinyoung Chun,[†] Jinwoo Lee,[†] and Jang H. Chun*,[‡]

Department of Chemical Engineering, Pohang University of Science and Technology, Pohang, Kyungbuk 790-784, Republic of Korea, and Department of Electronic Engineering, Kwangwoon University, Seoul 139-701, Republic of Korea

The phase-shift method and correlation constants, that is, unique electrochemical impedance spectroscopy (EIS) techniques for studying the linear relationship between the behavior ($-\varphi$ vs E) of the phase shift ($90° \geq -\varphi \geq 0°$) for the optimum intermediate frequency and that (θ vs E) of the fractional surface coverage ($0 \leq \theta \leq 1$), are proposed and verified to determine the Frumkin, Langmuir, and Temkin adsorption isotherms of overpotentially deposited hydrogen (OPD H) and related electrode kinetic and thermodynamic parameters of noble metals (alloys) in aqueous solutions. On Pt and Ir in 0.1 M KOH aqueous solution, the Frumkin and Temkin adsorption isotherms (θ vs E), equilibrium constants (K), interaction parameters (g), rates (r) of change of the standard free energy of OPD H with θ, and standard free energies (ΔG_θ^0) of OPD H are determined using the phase-shift method and correlation constants. The Frumkin adsorption isotherm is more accurate, useful, and effective than the Temkin adsorption isotherm. At $0.2 < \theta < 0.8$, the negative (positive) values of the interaction parameter for the Frumkin (Temkin) adsorption isotherms of OPD H are determined. A lateral attraction or repulsion interaction between the adsorbed OPD H species appears. The duality of the lateral attraction and repulsion interactions is probably a unique feature of OPD H on Pt, Ir, and Pt−Ir alloys in aqueous solutions.

Introduction

Many experimental methods have been used to study the adsorption of hydrogen for the cathodic H_2 evolution reaction (HER) on noble metals (alloys) in aqueous solutions. It is well-known that underpotentially deposited hydrogen (UPD H) and overpotentially deposited hydrogen (OPD H) occupy different surface adsorption sites and act as two distinguishable electroadsorbed H species and that only OPD H can contribute to the cathodic HER.[1−5] It is preferable to consider the Frumkin and Langmuir adsorption isotherms for OPD H rather than the equations of the electrode kinetics and thermodynamics for OPD H, because these adsorption isotherms are associated more directly with the atomic mechanism of OPD H.[6] However, there is not much reliable information on the Frumkin and Langmuir adsorption isotherms of OPD H and related electrode kinetic and thermodynamic data.

Many scientific phenomena have been interpreted by their behavior rather than by their nature. For example, the duality of light and electrons, that is, the wave and particle behaviors, is well-known in science and has been applied in engineering. Note that these wave and particle behaviors are not contradictory to each other but complementary. The phase-shift method and correlation constants are unique electrochemical impedance spectroscopy (EIS) techniques for studying the linear relationship between the behavior ($-\varphi$ vs E) of the phase shift ($90° \geq -\varphi \geq 0°$) for the optimum intermediate frequency (f_o) and that (θ vs E) of the fractional surface coverage ($0 \leq \theta \leq 1$) on noble metals (alloys) in aqueous solutions.[7−19] The behavior (θ vs E) of the fractional surface coverage ($0 \leq \theta \leq 1$) is well-known as the Frumkin or the Langmuir adsorption isotherm (θ vs E). The phase-shift method and correlation constants are also proposed and verified to determine the Frumkin and Temkin adsorption isotherms and related electrode kinetic and thermodynamic parameters of highly corrosion-resistant metals in aqueous solutions.[20,21]

New ideas or methods must be rigorously tested, especially when they are unique, but only with pure logic and objectivity and through scientific procedures. However, the objections to the phase-shift method in the comments[22−24] do not fulfill these criteria. These objections are substantially attributed to the confusion and misunderstanding about the newly defined equivalent circuit for the phase-shift method, the simplified equivalent circuit for intermediate frequencies, the linear relationship between $-\varphi$ versus E and θ versus E for f_o, and so forth. These rebuttals are clearly explained, stated, and summarized in the responses.[25,26] Note especially that all of the objections to the phase-shift method in the comment[24] are attributed to the confusion and misunderstanding about the applicability of related equations for intermediate frequencies and a unique feature of Faradaic resistances for recombination steps.[27] The validity and correctness of the phase-shift method should be discussed on the basis of simulations with a single equation for $-\varphi$ versus θ as a function of potential (E) and frequency (f) or relevant experimental results which are obtained using other conventional methods. The single equation for $-\varphi$ versus θ as a function of E and f has never been derived or discussed on the basis of relevant experimental results.[22−24] The simulations on the phase-shift method without this single equation are basically meaningless or in vain. Note that this

* To whom correspondence should be addressed. E-mail: jhchun@kw.ac.kr. Fax: +82-2-942-5235. Tel.: +82-2-940-5116.
[†] Pohang University of Science and Technology.
[‡] Kwangwoon University.

10.1021/je900805q
Published on Web 01/29/2010

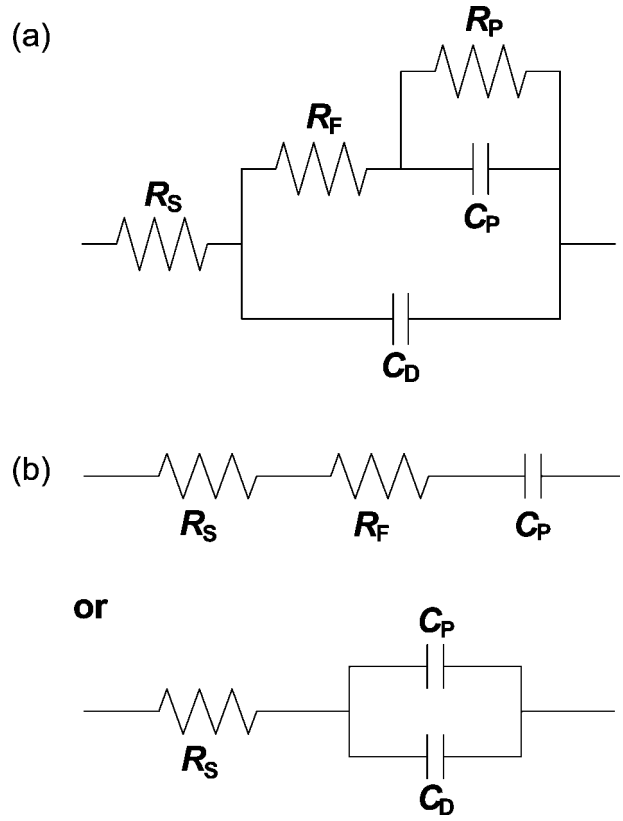

Figure 1. (a) Experimentally proposed equivalent circuit for the phase-shift method and (b) simplified equivalent circuit for the intermediate frequency responses. Equivalent circuit elements shown in Figure 1a are defined in this work.

problem has been experimentally and consistently solved using the phase-shift method for determining the adsorption isotherms.

In this paper, we represent the Frumkin and Temkin adsorption isotherms of OPD H and related electrode kinetic and thermodynamic parameters of Pt and Ir in 0.1 M KOH aqueous solution using the phase-shift method and correlation constants. The negative value of the interaction parameter for the Frumkin adsorption isotherms and the positive value of the interaction parameter for the Temkin adsorption isotherms of OPD H are determined. This aspect has not been frequently discussed on the basis of the relevant experimental results. This paper is the supplement to the previously published papers.[8,10,14,18,19]

Experimental Section

Preparations. Taking into account the H^+ concentration and effects of the diffuse double layer and pH,[28] an alkaline aqueous solution was prepared from KOH (Sigma-Aldrich, reagent grade) with purified water (resistivity: > 18 MΩ·cm) obtained from a Millipore system. The 0.1 M KOH aqueous solution (pH 12.99) was deaerated with 99.999 % purified nitrogen gas for 20 min before the experiments. A standard three-electrode configuration was employed. A saturated calomel electrode (SCE) was used as the standard reference electrode. A platinum wire (Johnson Matthey, purity: 99.9985 %, 1.0 mm diameter, estimated surface area: ca. 0.61 cm^2) and an iridium wire (Johnson Matthey, purity: 99.8 %, 1.0 mm diameter, estimated surface area: ca. 0.59 cm^2) were used as the working electrodes. A platinum wire (Johnson Matthey, purity: 99.95 %, 1.5 mm diameter) was used as the counter electrode. The Pt and Ir working electrodes were prepared by flame cleaning and then quenched and cooled in Millipore Milli-Q water and in air, sequentially.

Measurements. A cyclic voltammetry (CV) technique was used to achieve the steady state on Pt and Ir in 0.1 M KOH aqueous solution, respectively. The CV experiments were conducted for 25 cycles, with a scan rate of 200 $mV \cdot s^{-1}$ and a scan potential of (0 to −1.0) V versus the SCE for the adsorption of OPD H. After the CV experiments, an EIS technique was used to study the relation between the behavior ($-\varphi$ vs E) of the phase shift ($90° \geq -\varphi \geq 0°$) for the optimum intermediate frequency and that (θ vs E) of the fractional surface coverage ($0 \leq \theta \leq 1$) of OPD H on Pt and Ir in 0.1 M KOH aqueous solution, separately. The EIS experiments were conducted at scan frequencies of (10^4 to 0.5) Hz for high- and intermediate-frequency responses and (1 to 0.05) Hz for a low-frequency response, a single sine wave, an alternating current (ac) amplitude of 5 mV, and a direct current (dc) potential of (0 to −1.225) V versus the SCE for the adsorption of OPD H.

The CV experiments were performed using an EG & G Par model 273A potentiostat controlled with the Par model 270 software package. The EIS experiments were performed using the same apparatus in conjunction with a Schlumberger SI 1255 HF frequency response analyzer controlled with the Par model 398 software package. To obtain comparable and reproducible results, all measurements were carried out using the same preparations, procedures, and conditions at room temperature. The international sign convention is used, that is, cathodic currents and phase shifts or angles are taken as negative. To clarify the H adsorption in the different aqueous solutions, all potentials are given in the standard hydrogen electrode (SHE) scale. The Gaussian and adsorption isotherm analyses were carried out using the Excel and Origin software packages.

Results and Discussion

Theoretical and Experimental Backgrounds of the Phase-Shift Method. The equivalent circuit for the adsorption of OPD H for the cathodic HER on Pt and Ir in 0.1 M KOH aqueous solution, that is, at the Pt and Ir/0.1 M KOH aqueous solution interfaces, can be expressed as shown in Figure 1a.[29−31] Taking into account the superposition of various effects (relaxation time effects, real surface area problems, surface absorption and diffusion processes, inhomogeneous and lateral interactions, oxide layer formations, specific adsorptions, etc.) that are inevitable under the experimental measurements, we define the equivalent circuit elements. In Figure 1a, R_S is the aqueous solution resistance; R_F is the real resistance due to the Faradaic resistance (R_ϕ) for the discharge step and superposition of various effects; R_P is the real resistance due to the Faradaic resistance (R_R) for the recombination step and superposition of various effects; C_P is the real capacitance due to the adsorption pseudocapacitance (C_ϕ) and superposition of various effects; and C_D is the double-layer capacitance. Note that both R_ϕ and C_ϕ are not constant but dependent on E and θ and cannot be measured. Both R_F and C_P are not constant but dependent on E and θ and can be measured.

The numerical derivation of C_ϕ from the Frumkin and Langmuir adsorption isotherms (θ vs E) is described elsewhere, and R_ϕ depends on C_ϕ.[29,30] A unique feature of R_ϕ and C_ϕ attaining maximum values at $\theta \approx 0.5$ and intermediate E, decreasing symmetrically with E at other values of θ, and approaching minimum values at $\theta \approx 0$ and low E and $\theta \approx 1$ and high E is well-known in interfacial electrochemistry, electrode kinetics, and EIS. The unique feature and combination of R_ϕ and C_ϕ versus E imply that the normalized change rate of $-\varphi$ versus E, that is, $\Delta(-\varphi)/\Delta E$, corresponds to that of θ versus E, that is, $\Delta\theta/\Delta E$, and vice versa. Both $\Delta(-\varphi)/\Delta E$ and $\Delta\theta/\Delta E$

Table 1. Measured Values of the Phase Shift ($-\varphi$) for the Optimum Intermediate Frequency ($f_o = 1.259$ Hz), the Estimated Fractional Surface Coverage (θ) of OPD H, and the Normalized Change Rates ($\Delta(-\varphi)/\Delta E$ and $\Delta\theta/\Delta E$) on Pt in 0.1 M KOH Aqueous Solution

E/V vs SHE	$-\varphi$/deg	θ ($0 \le \theta \le 1$)	$\Delta(-\varphi)$, $\Delta\theta/\Delta E$
−0.609	87.5	≈ 0	≈ 0
−0.634	87.1	0.004598	0.055172
−0.659	86.9	0.006897	0.027586
−0.684	82.8	0.054023	0.565517
−0.709	67.8	0.226437	2.068966
−0.734	33.3	0.622989	4.758621
−0.759	11.0	0.879310	3.075862
−0.784	4.1	0.958621	0.951724
−0.809	2.1	0.981609	0.275862
−0.834	1.4	0.989655	0.096552
−0.859	0.9	0.995402	0.068966
−0.884	0.6	0.998851	0.041379
−0.909	0.5	≈ 1	0.013793

Table 2. Measured Values of the Phase Shift ($-\varphi$) for the Optimum Intermediate Frequency ($f_o = 1.259$ Hz), the Estimated Fractional Surface Coverage (θ) of OPD H, and the Normalized Change Rates ($\Delta(-\varphi)/\Delta E$, $\Delta\theta/\Delta E$) on Ir in 0.1 M KOH Aqueous Solution

E/V vs SHE	$-\varphi$/deg	θ ($0 \le \theta \le 1$)	$\Delta(-\varphi)$, $\Delta\theta/\Delta E$
−0.659	71.6	≈ 0	≈ 0
−0.684	70.3	0.018705	0.187050
−0.709	60.5	0.159712	1.410072
−0.734	34.8	0.529496	3.697842
−0.759	13.8	0.831655	3.021583
−0.784	5.7	0.948201	1.165468
−0.809	3.4	0.981295	0.330935
−0.834	3.0	0.987050	0.057554
−0.859	2.5	0.994245	0.071942
−0.884	2.4	0.995683	0.014388
−0.909	2.1	≈ 1	0.043165

are maximized at $\theta \approx 0.5$ and intermediate E, decrease symmetrically with E at other values of θ, and are minimized at $\theta \approx 0$ and low E and $\theta \approx 1$ and high E. This is not a mere coincidence but a unique feature of the Frumkin and Langmuir adsorption isotherms. The Gaussian profile and linear relationship between $\Delta(-\varphi)/\Delta E$ and $\Delta\theta/\Delta E$ most clearly appear at the optimum intermediate frequency (f_o). The determination of f_o is experimentally and graphically evaluated on the basis of $\Delta(-\varphi)/\Delta E$ and $\Delta\theta/\Delta E$ for intermediate and other frequencies (see Figures 6 and 7). The importance of f_o is described elsewhere.[18] These aspects are the essential nature of the phase-shift method for determining the Frumkin and Langmuir adsorption isotherms.

The frequency responses of the equivalent circuit for all f shown in Figure 1a are essential for understanding the unique feature and combination of R_ϕ and C_ϕ versus E for f_o, that is, the Gaussian profile and linear relationship between $-\varphi$ versus E and θ versus E for f_o. At very low frequencies, the equivalent circuit for all f shown in Figure 1a can be expressed as a series circuit of R_S, R_F, and R_P. At very high frequencies, the equivalent circuit for all f shown in Figure 1a can be expressed as a series circuit of R_S and C_D. At intermediate frequencies, one finds regions in which the equivalent circuit for all f shown in Figure 1a behaves as a series circuit of R_S, R_F, and C_P or a series and parallel circuit of R_S, C_P, and C_D as shown in Figure 1b.[29,30] However, note that the simplified equivalent circuit shown in Figure 1b does not represent the change of the cathodic HER itself but only the intermediate frequency response.

In Figure 1b, the impedance (Z) and phase shift ($-\varphi$) for intermediate frequencies are given by

$$Z = (R_S + R_F) - j/\omega C_P \quad (1a)$$

$$-\varphi = \arctan[1/\omega(R_S + R_F)C_P] \quad (1b)$$

or

$$Z = R_S - j/\omega(C_P + C_D) \quad (2a)$$

$$-\varphi = \arctan[1/\omega R_S(C_P + C_D)] \quad (2b)$$

$R_P \gg 1/\omega C_P$ and $(R_S + R_F)$

$$R_F \propto R_\phi \text{ and } C_P \propto C_\phi \text{ and } R_\phi \propto C_\phi \quad (3)$$

where j is an operator and is equal to the square root of -1, that is, $j^2 = -1$, ω ($= 2\pi f$) is the angular frequency, and f is the frequency. In our previously published papers, only eq 1 is used with a footnote, that is, C_P practically includes C_D (see Tables 1 and 2 in ref 17, Table 1 in ref 16, etc.). Both eqs 1 and 2 show that the effect of R_P on $-\varphi$ for intermediate frequencies is negligible. These aspects are completely overlooked, confused, and misunderstood in the comments on the phase-shift method by Horvat-Radosevic, Kvastek, and Lasia.[22−24] Correspondingly, all of the simulations on the phase-shift method using eq 1, which appears in the comments (C_P does not include C_D),[22−24] are basically invalid or wrong.[27] All of the analyses of the effect of R_P on $-\varphi$ for intermediate frequencies are also invalid or wrong.

The following limitations and conditions of the equivalent circuit elements for f_o are summarized on the basis of the experimental data.[7−21] Both R_S and C_D are not constant. At $\theta \approx 0$, $R_S > R_F$ and $C_D > C_P$, vice versa, and so forth. For a wide range of θ, that is, $0.2 < \theta < 0.8$, $R_F \gg R_S$ or $R_F > R_S$ and $C_P \gg C_D$ or $C_P > C_D$, and so forth. At $\theta \approx 1$, $R_S > R_F$ or $R_S < R_F$ and $C_P \gg C_D$. The measured $-\varphi$ for f_o depends on E and θ. In contrast to numerical calculations or analyses, these limitations and conditions for eq 1 or 2 are not considered. At intermediate frequencies, all of the measured $-\varphi$ include (R_S, R_F) and (C_P, C_D). Therefore, the measured $-\varphi$ for f_o is valid and correct regardless of the applicability of eq 1 or 2 and the related limitations and conditions. This is the reason why the phase-shift method is probably the most useful and effective way to determine the adsorption isotherms. The combination of (R_S, R_F) and (C_P, C_D) is equivalent to that of R_ϕ and C_ϕ. This is attributed to the reciprocal property of R_F and C_P.[7−21] As stated above, the unique feature and combination of R_ϕ and C_ϕ versus E, that is, $\Delta(-\varphi)/\Delta E$ and $\Delta\theta/\Delta E$, most clearly appear at f_o. The Gaussian profile and linear relationship between $\Delta(-\varphi)/\Delta E$ and $\Delta\theta/\Delta E$ for f_o imply that only one Frumkin or Langmuir adsorption isotherm is determined on the basis of the relevant experimental results (see Figures 6 to 9). This is another reason why the phase-shift method is probably the most accurate way to determine the adsorption isotherms.

Basic Procedure and Description of the Phase-Shift Method. Figure 2 compares the phase-shift curves ($-\varphi$ vs log f) for different potentials (E) on Pt in 0.1 M KOH aqueous solution. The intermediate frequency, that is, a vertical solid line (1.259 Hz) on $-\varphi$ versus log f shown in Figure 2, can be set as f_o for $-\varphi$ versus E and θ versus E. At the maximum $-\varphi$ shown in Figure 2a, it appears that the adsorption of OPD H and superposition of various effects are minimized, that is, $\theta \approx 0$ and E is low. Note that θ ($0 \le \theta \le 1$) depends on E. At the maximum $-\varphi$, when $\theta \approx 0$ and E is low, both $\Delta(-\varphi)/\Delta E$ and $\Delta\theta/\Delta E$ are minimized because of R_ϕ and C_ϕ approaching minimum values. At the minimum $-\varphi$ shown in Figure 2m, it appears that the adsorption of OPD H and superposition of various effects are maximized or almost saturated, that is, $\theta \approx 1$ and E is high. At the minimum $-\varphi$, when $\theta \approx 1$ and E is

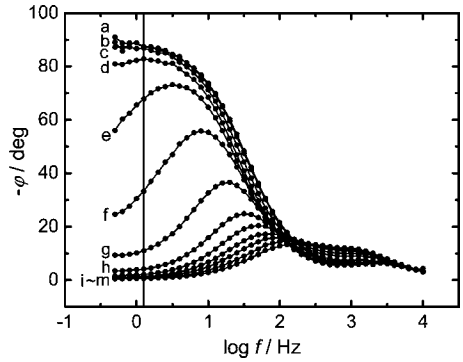

Figure 2. Comparison of the phase-shift curves ($-\varphi$ vs log f) for different potentials (E) on Pt in 0.1 M KOH aqueous solution. Measured value: ●. Vertical solid line indicates 1.259 Hz; single sine wave; scan frequency of (10^4 to 0.5) Hz; ac amplitude: 5 mV; dc potential: (a) −0.609 V, (b) −0.634 V, (c) −0.659 V, (d) −0.684 V, (e) −0.709 V, (f) −0.734 V, (g) −0.759 V, (h) −0.784 V, (i) −0.809 V, (j) −0.834 V, (k) −0.859 V, (l) −0.884 V, and (m) −0.909 V versus SHE.

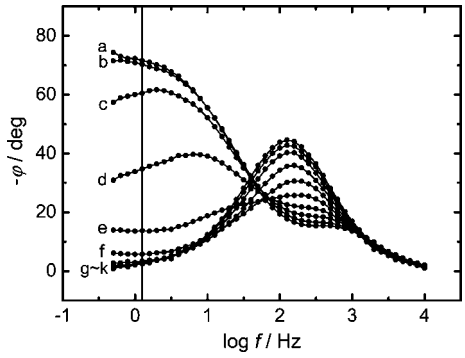

Figure 3. Comparison of the phase-shift curves ($-\varphi$ vs log f) for different potentials (E) on Ir in 0.1 M KOH aqueous solution. Measured value: ●. Vertical solid line indicates 1.259 Hz; single sine wave; scan frequency: (10^4 to 0.5) Hz; ac amplitude: 5 mV; dc potential: (a) −0.659 V, (b) −0.684 V, (c) −0.709 V, (d) −0.734 V, (e) −0.759 V, (f) −0.784 V, (g) −0.809 V, (h) −0.834 V, (i) −0.859 V, (j) −0.884 V, and (k) −0.909 V versus SHE.

high, both $\Delta(-\varphi)/\Delta E$ and $\Delta\theta/\Delta E$ are also minimized because of R_ϕ and C_ϕ approaching minimum values. At the medium $-\varphi$ between parts e and f of Figure 2, it appears that both $\Delta(-\varphi)/\Delta E$ and $\Delta\theta/\Delta E$ are maximized because of R_ϕ and C_ϕ approaching maximum values at $\theta \approx 0.5$ and intermediate E.

Figure 3 compares the phase-shift curves ($-\varphi$ vs log f) for different potentials (E) on Ir in 0.1 M KOH aqueous solution. The intermediate frequency, that is, a vertical solid line (1.259 Hz) on $-\varphi$ versus log f shown in Figure 3, can be set as f_o for $-\varphi$ versus E and θ versus E. At the maximum $-\varphi$ shown in Figure 3a, it appears that the adsorption of OPD H and superposition of various effects are minimized, that is, $\theta \approx 0$ and E is low. As stated above, θ ($0 \le \theta \le 1$) depends on E. At the maximum $-\varphi$, when $\theta \approx 0$ and E is low, both $\Delta(-\varphi)/\Delta E$ and $\Delta\theta/\Delta E$ are minimized because of R_ϕ and C_ϕ approaching minimum values. At the minimum $-\varphi$ shown in Figure 3k, it appears that the adsorption of OPD H and superposition of various effects are maximized or almost saturated, that is, $\theta \approx 1$ and E is high. At the minimum $-\varphi$, when $\theta \approx 1$ and E is high, both $\Delta(-\varphi)/\Delta E$ and $\Delta\theta/\Delta E$ are also minimized because of R_ϕ and C_ϕ approaching minimum values. At the medium $-\varphi$ between parts c and d of Figure 3, it appears that both $\Delta(-\varphi)/\Delta E$ and $\Delta\theta/\Delta E$ are maximized because of R_ϕ and C_ϕ approaching maximum values at $\theta \approx 0.5$ and intermediate E.

The procedure and description of the phase-shift method for OPD H on Pt and Ir in 0.1 M KOH aqueous solution are briefly

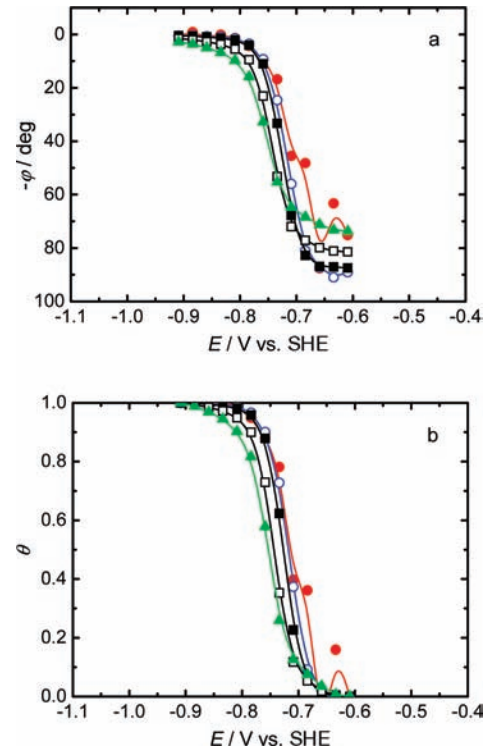

Figure 4. Comparison of (a) the phase-shift profiles ($-\varphi$ vs E) and (b) surface-coverage profiles (θ vs E) for five different frequencies on Pt in 0.1 M KOH aqueous solution. Measured or estimated values: ●, 0.1 Hz; ○, 0.5 Hz; ■, 1.259 Hz; □, 5.012 Hz; ▲, 10 Hz. The optimum intermediate frequency (f_o) is 1.259 Hz (■).

summarized in Tables 1 and 2, respectively. Tables 1 and 2 show the changes of $-\varphi$ versus E and θ versus E for f_o (= 1.259 Hz) with 25 mV increment changes in negative potential (E) on Pt and Ir in 0.1 M KOH aqueous solution, respectively. The changes of $-\varphi$ versus E and θ versus E for f_o (= 1.259 Hz) illustrated in Figures 4 and 5 are obtained on the basis of the experimental results summarized in Tables 1 and 2, respectively. The changes of $-\varphi$ versus E and θ versus E for other frequencies (0.1 Hz, 0.5 Hz, 5.012 Hz, and 10 Hz) illustrated in Figures 4 and 5 are also obtained through the same procedure summarized in Tables 1 and 2, respectively.

As shown in Figures 2 and 3, $-\varphi$ depends on both f and E. The adsorption of OPD H, that is, θ, depends on only E. As previously described, the Gaussian profile and linear relationship between $\Delta(-\varphi)/\Delta E$ and $\Delta\theta/\Delta E$ most clearly appear at f_o. This is the reason why the comparison of $-\varphi$ versus E and θ versus E for different frequencies shown in Figures 4 and 5 is necessary to determine f_o. Note that $-\varphi$ versus E shown in Figures 4a and 5a corresponds to θ versus E shown in Figures 4b and 5b and vice versa, respectively. The difference between $-\varphi$ versus E and θ versus E for f_o (= 1.259 Hz) and other frequencies (0.1 Hz, 0.5 Hz, 5.012 Hz, and 10 Hz) shown in Figures 4 and 5 does not represent the measurement error but only the frequency response.

Under the same conditions, the adsorption features of hydrogen and oxygen on Pt and Ir are different from each other even though both Pt and Ir belong to the platinum group of metals (see Figure 1 in ref 14 and Figure 1 in ref 12). Similarly, the adsorption feature of OPD H on Pt and Ir is different from each other.[1−5] Figures 4 and 5 also show that the adsorption feature of OPD H, that is, $-\varphi$ versus E and θ versus E for f_o (= 1.259 Hz), on Pt and Ir is different from each other. As previously described, theoretical analyses of $-\varphi$ versus θ as a function of E and f have never been discussed elsewhere.

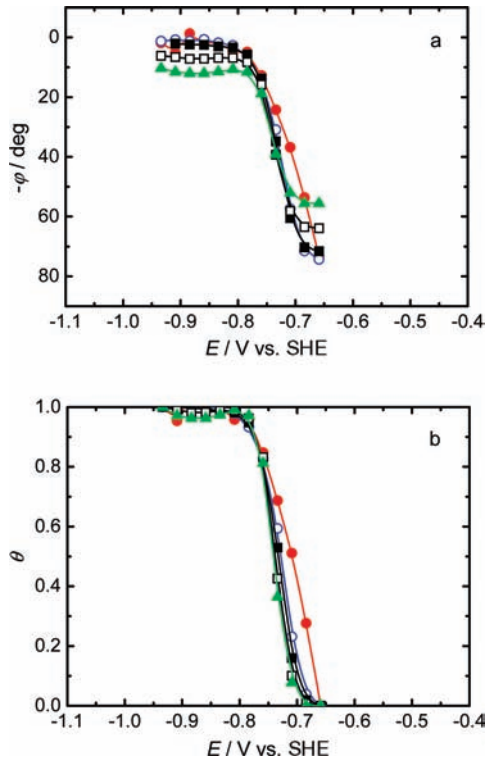

Figure 5. Comparison of (a) the phase-shift profiles ($-\varphi$ vs E) and (b) surface-coverage profiles (θ vs E) for five different frequencies on Ir in 0.1 M KOH aqueous solution. Measured or estimated values: ●, 0.1 Hz; ○, 0.5 Hz; ■, 1.259 Hz; □, 5.012 Hz; ▲, 10 Hz. The optimum intermediate frequency (f_o) is 1.259 Hz (■).

Figures 6 and 7 compare the normalized change rates of $-\varphi$ versus E and θ versus E, $\Delta(-\varphi)/\Delta E$ and $\Delta\theta/\Delta E$, for five different frequencies on Pt and Ir in 0.1 M KOH aqueous solution, respectively. Note that $\Delta(-\varphi)/\Delta E$ and $\Delta\theta/\Delta E$ shown in Figures 6 and 7 correspond to $-\varphi$ versus E and θ versus E shown in Figures 4 and 5 and vice versa, respectively. The Gaussian profiles of $\Delta(-\varphi)/\Delta E$ and $\Delta\theta/\Delta E$ for f_o (= 1.259 Hz) shown in Figures 6c and 7c are illustrated on the basis of the experimental results summarized in Tables 1 and 2, respectively. Similarly, the Gaussian profiles of $\Delta(-\varphi)/\Delta E$ and $\Delta\theta/\Delta E$ for other frequencies (0.1 Hz, 0.5 Hz, 5.012 Hz, and 10 Hz) shown in Figures 6 and 7 are illustrated through the same procedure summarized in Tables 1 and 2, respectively. In Figures 6c and 7c, $\Delta(-\varphi)/\Delta E$ corresponds to $\Delta\theta/\Delta E$ and vice versa. Both $\Delta(-\varphi)/\Delta E$ and $\Delta\theta/\Delta E$ are maximized at the medium $-\varphi$, when $\theta \approx 0.5$ and E is intermediate, decrease symmetrically with E at other values of θ, and are minimized at the maximum $-\varphi$, when $\theta \approx 0$ and E is low, and the minimum $-\varphi$, when $\theta \approx 1$ and E is high. As previously described, this is a unique feature of the Frumkin and Langmuir adsorption isotherms. Figures 6a and 7a show that the low frequency response, that is, the effect of R_P on $-\varphi$, appears at 0.1 Hz. The difference between the Gaussian profiles of $\Delta(-\varphi)/\Delta E$ and $\Delta\theta/\Delta E$ for f_o (= 1.259 Hz) and other frequencies (0.1 Hz, 0.5 Hz, 5.012 Hz, and 10 Hz) shown in Figures 6 and 7 does not represent the measurement error but only the frequency response.

Finally, one can conclude that the three regions, that is, (maximum $-\varphi$, $\theta \approx 0$, low E), (medium $-\varphi$, $\theta \approx 0.5$, intermediate E), and (minimum $-\varphi$, $\theta \approx 1$, high E), the Gaussian profile, and the corresponding Frumkin or Langmuir adsorption isotherm are readily determined on the basis of $\Delta(-\varphi)/\Delta E$ and $\Delta\theta/\Delta E$ for f_o (see Tables 1 and 2 and Figures 4 to 9). The Gaussian profile and linear relationship between $\Delta(-\varphi)/\Delta E$ and $\Delta\theta/\Delta E$ for f_o express the essential nature of the phase-shift method for determining the Frumkin or the Langmuir adsorption isotherm. This is not valid and correct for all f and E, but only for f_o and a limited range of E. This is another reason why the phase-shift method is probably the most accurate way to determine the adsorption isotherms.

Frumkin, Langmuir, and Temkin Adsorption Isotherms. The derivation and interpretation of the practical forms of the electrochemical Frumkin, Langmuir, and Temkin adsorption isotherms are described elsewhere.[32−34] The Frumkin adsorption isotherm assumes that the electrode surface is inhomogeneous or that the lateral interaction effect is not negligible. The Frumkin adsorption isotherm of OPD H can be expressed as follows[33]

$$[\theta/(1-\theta)]\exp(g\theta) = K_o C_H^+ [\exp(-EF/RT)] \quad (4)$$

$$g = r/RT \quad (5)$$

$$K = K_o \exp(-g\theta) \quad (6)$$

where θ ($0 \le \theta \le 1$) is the fractional surface coverage of OPD H, g is the interaction parameter for the Frumkin adsorption isotherm, K_o is the equilibrium constant for OPD H at $g = 0$, C_H^+ is the H^+ concentration in the bulk solution, E is the negative potential, F is Faraday's constant, R is the gas constant, T is the absolute temperature, r is the rate of change of the standard free energy of OPD H with θ ($0 \le \theta \le 1$), and K is the equilibrium constant for OPD H. The dimension of K is described elsewhere.[35] Note that $g = 0$ in eqs 4 to 6, which implies the Langmuir adsorption isotherm. For the Langmuir adsorption isotherm, when $g = 0$, the inhomogeneous and lateral interaction effects on the adsorption of OPD H are negligible.

On Pt in 0.1 M KOH aqueous solution, the numerically calculated Frumkin adsorption isotherms using eq 4 are shown in Figure 8. Parts a, b, and c of Figure 8 show the three numerically calculated Frumkin adsorption isotherms corresponding to $g = 0$, -2.4, and -7.2, respectively, for $K_o = 1.2 \cdot 10^{-4}$ mol^{-1}. Note that $g = 0$ for $K_o = 1.2 \cdot 10^{-4}$ mol^{-1} shown in Figure 8a, which implies the Langmuir adsorption isotherm, that is, $K = 1.2 \cdot 10^{-4}$ mol^{-1}. The Frumkin adsorption isotherm, $K = 1.2 \cdot 10^{-4} \exp(2.4\theta)$ mol^{-1}, shown in Figure 8b is applicable to the adsorption of OPD H. Using eq 5, r is -6.0 kJ·mol^{-1}.

On Ir in 0.1 M KOH aqueous solution, the numerically calculated Frumkin adsorption isotherms using eq 4 are shown in Figure 9. Parts a, b and c of Figure 9 show the three numerically calculated Frumkin adsorption isotherms corresponding to $g = 0$, -2.4, and -7.2, respectively, for $K_o = 9.4 \cdot 10^{-5}$ mol^{-1}. Note that $g = 0$ for $K_o = 9.4 \cdot 10^{-5}$ mol^{-1} shown in Figure 9a, which implies the Langmuir adsorption isotherm, that is, $K = 9.4 \cdot 10^{-5}$ mol^{-1}. The Frumkin adsorption isotherm, $K = 9.4 \cdot 10^{-5} \exp(2.4\theta)$ mol^{-1}, shown in Figure 9b is applicable to the adsorption of OPD H. Using eq 5, r is -6.0 kJ·mol^{-1}.

At intermediate values of θ, that is, $0.2 < \theta < 0.8$, the pre-exponential term, $[\theta/(1-\theta)]$, varies little with θ compared to the variation of the exponential term, $\exp(g\theta)$ (see eq 4). Under the approximate conditions, the Temkin adsorption isotherm can be simply derived from the Frumkin adsorption isotherm. The Temkin adsorption isotherm of OPD H can be expressed as follows[33]

$$\exp(g\theta) = K_o C_H^+ [\exp(-EF/RT)] \quad (7)$$

Figure 10 shows the determination of the Temkin adsorption isotherm correlating with the Frumkin adsorption isotherm shown in Figure 8b. In Figure 10b, the numerically calculated Temkin adsorption isotherm using eq 7 is $K = 1.2 \cdot 10^{-3}$

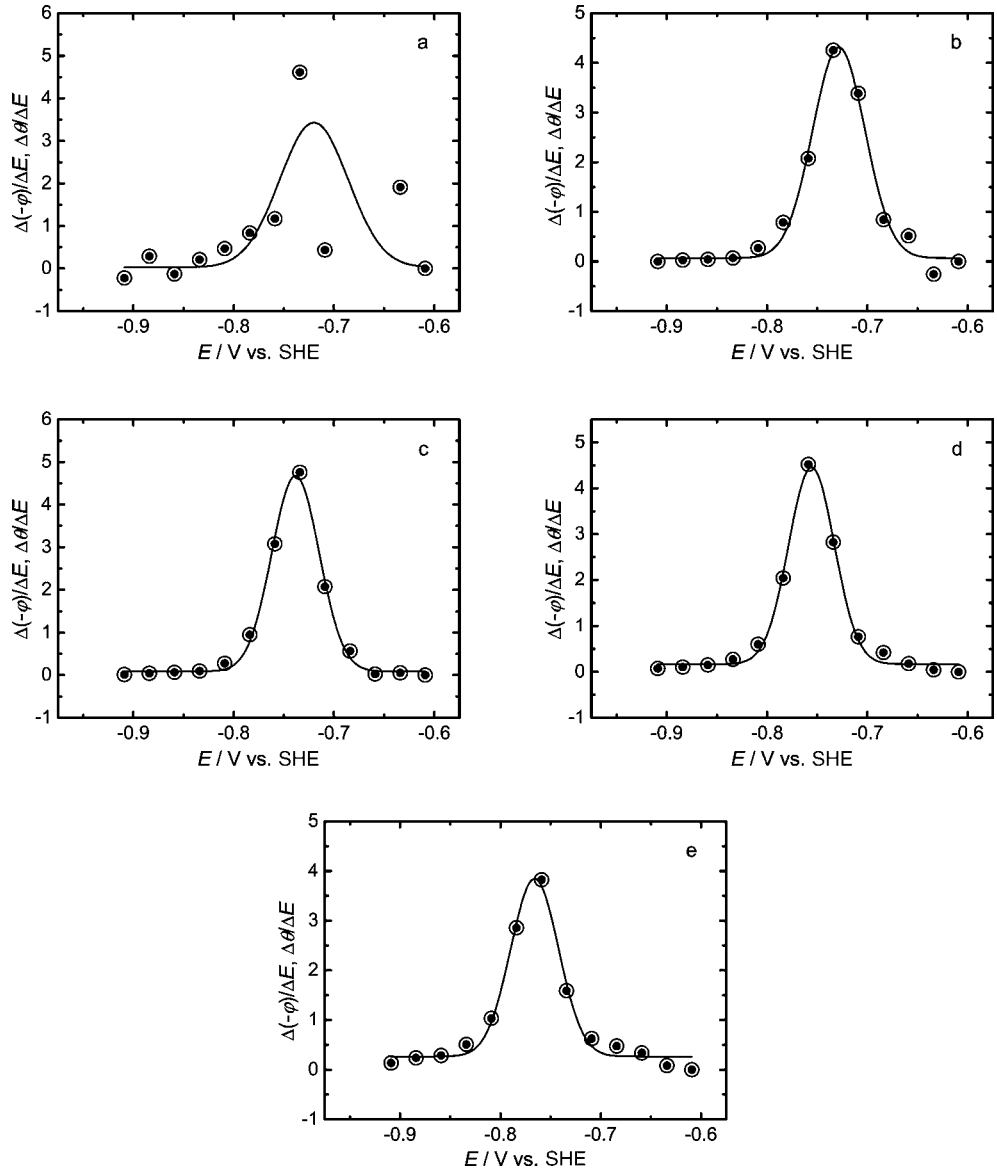

Figure 6. Comparison of the normalized change rates of $-\varphi$ versus E and θ versus E, $\Delta(-\varphi)/\Delta E$ and $\Delta\theta/\Delta E$, for five different frequencies on Pt in 0.1 M KOH aqueous solution. Solid line indicates the fitted Gaussian profile. ○, $\Delta(-\varphi)/\Delta E$; ●, $\Delta\theta/\Delta E$; (a) 0.1 Hz, (b) 0.5 Hz, (c) 1.259 Hz, (d) 5.012 Hz, and (e) 10 Hz. The optimum intermediate frequency (f_o) is 1.259 Hz.

$\exp(-2.2\theta)$ mol^{-1}. Using eq 5, r is 5.5 $kJ \cdot mol^{-1}$. Note that the Temkin adsorption isotherm shown in Figure 10b is only valid and effective at $0.2 < \theta < 0.8$.

Figure 11 shows the determination of the Temkin adsorption isotherm correlating with the Frumkin adsorption isotherm shown in Figure 9b. In Figure 11b, the numerically calculated Temkin adsorption isotherm using eq 7 is $K = 9.4 \cdot 10^{-4}$ $\exp(-2.2\theta)$ mol^{-1}. Using eq 5, r is 5.5 $kJ \cdot mol^{-1}$. Note that the Temkin adsorption isotherm shown in Figure 11b is only valid and effective at $0.2 < \theta < 0.8$.

Correlation Constants between the Adsorption Isotherms. As previously described, the Frumkin, Langmuir, and Temkin adsorption conditions are different from each other. Only one Frumkin adsorption isotherm is determined on the basis of the relevant experimental results (see Figures 8 and 9). However, as shown in Figures 10 and 11, the two different adsorption isotherms, that is, the Temkin and Frumkin adsorption isotherms, appear to fit the same data at $0.2 < \theta < 0.8$ (also see Supplementary Figures 1 and 2 in the Supporting Information). This unique feature of the Temkin and Frumkin or Langmuir adsorption isotherms has been experimentally and consistently verified using the phase-shift method and correlation constants.[16−21]

In this work, one can also confirm that the Temkin adsorption isotherm correlating with the Frumkin or the Langmuir adsorption isotherm, and vice versa, is readily determined using the correlation constants. At $0.2 < \theta < 0.8$, the two different adsorption isotherms, that is, the Temkin and Frumkin or Langmuir adsorption isotherms, appear to fit the same data regardless of their adsorption conditions. The values of g and K_o for the Temkin adsorption isotherm are approximately 4.6 and 10 times greater than those for the correlating Frumkin or Langmuir adsorption isotherm, respectively. This aspect is described elsewhere.[16,17,20]

Lateral Attraction and Repulsion Interactions. A negative value of the interaction parameter (g) for the Frumkin adsorption isotherm is qualitatively and quantitatively interpreted elsewhere.[36] The negative value of g for the Frumkin adsorption isotherms shown in Figures 8b and 9b implies a lateral attraction interaction between the adsorbed OPD H species, that is, an increase of the standard free energy of OPD H with θ ($0 \leq \theta$

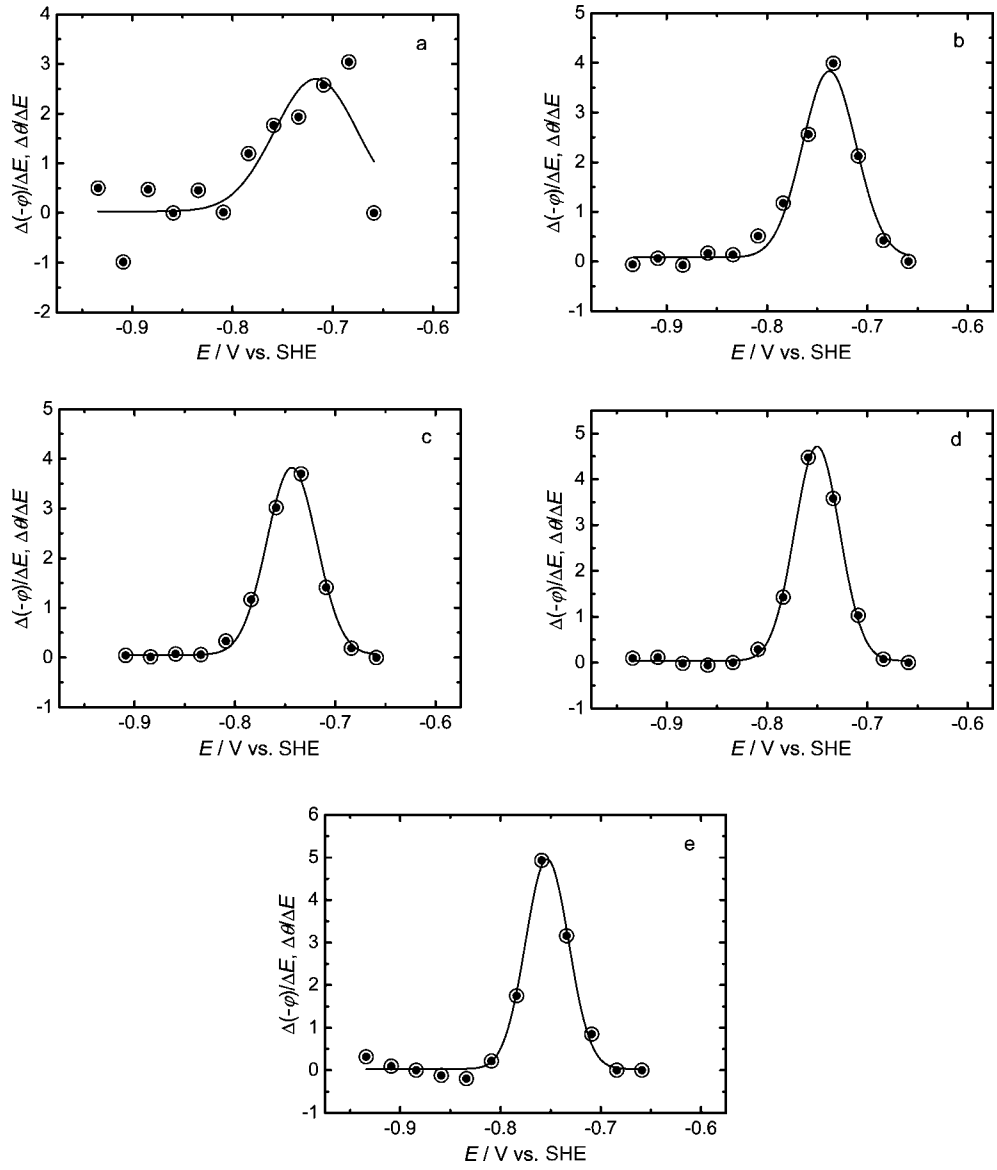

Figure 7. Comparison of the normalized change rates of $-\varphi$ versus E and θ versus E, $\Delta(-\varphi)/\Delta E$ and $\Delta\theta/\Delta E$, for five different frequencies on Ir in 0.1 M KOH aqueous solution. Solid line indicates the fitted Gaussian profile. ○, $\Delta(-\varphi)/\Delta E$; ●, $\Delta\theta/\Delta E$; (a) 0.1 Hz, (b) 0.5 Hz, (c) 1.259 Hz, (d) 5.012 Hz, and (e) 10 Hz. The optimum intermediate frequency (f_o) is 1.259 Hz.

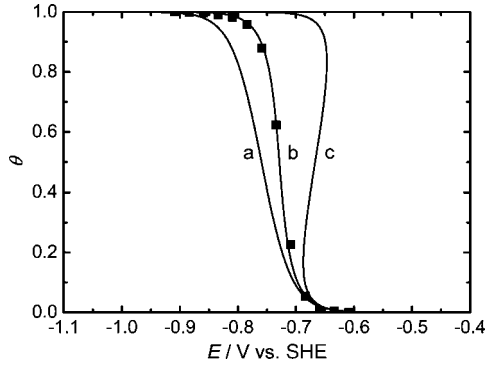

Figure 8. Comparison of the experimental and fitted data for the Frumkin adsorption isotherms (θ vs E) of OPD H on Pt in 0.1 M KOH aqueous solution. Experimental data: ■. Calculated value using eq 4: —. (a) $g = 0$, (b) $g = -2.4$, and (c) $g = -7.2$ for $K_o = 1.2 \cdot 10^{-4}$ mol^{-1}. Using eqs 4 to 6, (a) $g = 0$ for $K_o = 1.2 \cdot 10^{-4}$ mol^{-1}, which is the Langmuir adsorption isotherm, that is, $K = 1.2 \cdot 10^{-4}$ mol^{-1}.

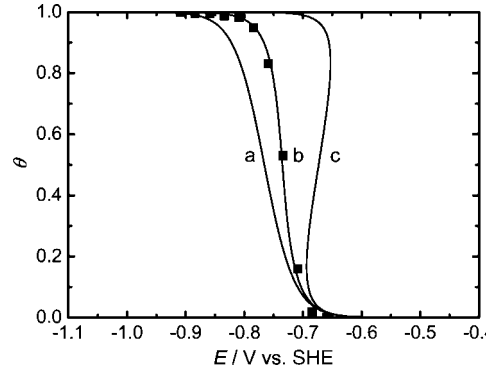

Figure 9. Comparison of the experimental and fitted data for the Frumkin adsorption isotherms (θ vs E) of OPD H on Ir in 0.1 M KOH aqueous solution. Experimental data: ■. Calculated value using eq 4: —. (a) $g = 0$, (b) $g = -2.4$, and (c) $g = -7.2$ for $K_o = 9.4 \cdot 10^{-5}$ mol^{-1}. Using eqs 4 to 6, (a) $g = 0$ for $K_o = 9.4 \cdot 10^{-5}$ mol^{-1}, which is the Langmuir adsorption isotherm, that is, $K = 9.4 \cdot 10^{-5}$ mol^{-1}.

≤ 1). This interaction is probably the unique feature of the Frumkin adsorption isotherms of OPD H on Pt, Ir, and Pt−Ir alloys in aqueous solutions.[19] On the other hand, the positive value of g for the Temkin adsorption isotherms shown in Figures

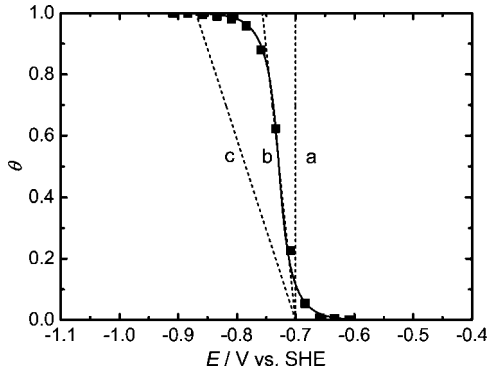

Figure 10. Comparison of the experimentally determined Frumkin adsorption isotherm and three fitted Temkin adsorption isotherms (θ vs E) of OPD H on Pt in 0.1 M KOH aqueous solution. Experimental data: ■. Calculated value using eq 4 (Frumkin adsorption isotherm): —. Calculated value using eq 7 (Temkin adsorption isotherm): ----. (a) $g = 0$, (b) $g = 2.2$, and (c) $g = 6.6$ for $K_o = 1.2 \cdot 10^{-3}$ mol^{-1}. In Figure 10b, the Temkin adsorption isotherm, $K = 1.2 \cdot 10^{-3} \exp(-2.2\theta)$ mol^{-1}, is only valid and effective at $0.2 < \theta < 0.8$.

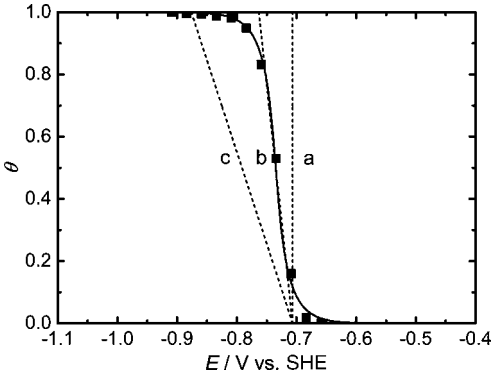

Figure 11. Comparison of the experimentally determined Frumkin adsorption isotherm and three fitted Temkin adsorption isotherms (θ vs E) of OPD H on Ir in 0.1 M KOH aqueous solution. Experimental data: ■. Calculated value using eq 4 (Frumkin adsorption isotherm): —. Calculated value using eq 7 (Temkin adsorption isotherm): ----. (a) $g = 0$, (b) $g = 2.2$, and (c) $g = 6.6$ for $K_o = 9.4 \cdot 10^{-4}$ mol^{-1}. In Figure 11b, the Temkin adsorption isotherm, $K = 9.4 \cdot 10^{-4} \exp(-2.2\theta)$ mol^{-1}, is only valid and effective at $0.2 < \theta < 0.8$.

10b and 11b implies a lateral repulsion interaction between the adsorbed OPD H species, that is, a decrease of the standard free energy of OPD H with θ ($0.2 < \theta < 0.8$).

On the basis of the correlation constants between the adsorption isotherms,[16−21] from the negative ($g < 0$) and positive ($g > 0$) values of g presented in refs 17 to 19 and Figures 10 and 11 in this work, one can interpret that the lateral attraction ($g < 0$) or repulsion ($g > 0$) interaction between the adsorbed OPD H species appears at $0.2 < \theta < 0.8$. As shown in Figures 10b and 11b (also see Supplementary Figures 1b and 2b in the Supporting Information), the region ($0.2 < \theta < 0.8$) corresponds to a short potential range (ca. 34 mV). Consequently, one can interpret that the observation of the lateral attraction or repulsion interaction between the adsorbed OPD H species is difficult using other conventional methods. The duality of the lateral attraction and repulsion interactions is probably a unique feature of OPD H on Pt, Ir, and Pt−Ir alloys in aqueous solutions.[19]

Applicability of the Temkin Adsorption Isotherm. Figures 12 and 13 show the applicability of the Frumkin and Temkin adsorption isotherms of OPD H on Pt and Ir in 0.1 M KOH aqueous solution at the same potential range, respectively. As shown in Figures 10b and 11b (also see Supplementary Figures 1b and 2b in the Supporting Information), the Temkin adsorption

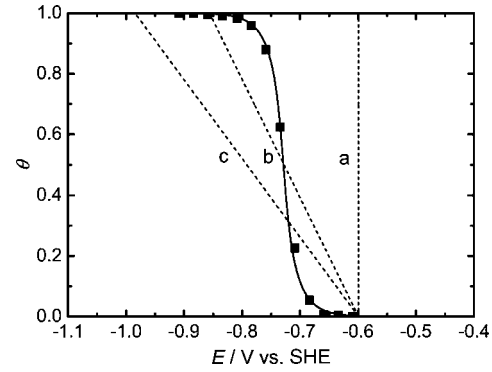

Figure 12. Evaluation of the applicability of the Frumkin and Temkin adsorption isotherms (θ vs E) of OPD H on Pt in 0.1 M KOH aqueous solution at the same potential range. Experimental data: ■. Calculated value using eq 4 (Frumkin adsorption isotherm): —. Calculated value using eq 7 (Temkin adsorption isotherm): ----. (a) $g = 0$, (b) $g = 10$, and (c) $g = 15$ for $K_o = 6.1 \cdot 10^{-2}$ mol^{-1}.

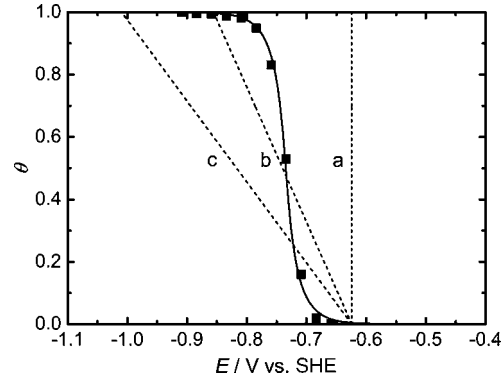

Figure 13. Evaluation of the applicability of the Frumkin and Temkin adsorption isotherms (θ vs E) of OPD H on Ir in 0.1 M KOH aqueous solution at the same potential range. Experimental data: ■. Calculated value using eq 4 (Frumkin adsorption isotherm): —. Calculated value using eq 7 (Temkin adsorption isotherm): ----. (a) $g = 0$, (b) $g = 9$, and (c) $g = 15$ for $K_o = 2.3 \cdot 10^{-2}$ mol^{-1}.

isotherm is only valid and effective at $0.2 < \theta < 0.8$. The short potential range (ca. 34 mV) is difficult to observe in the Temkin adsorption isotherm correlating with the Frumkin adsorption isotherm. At other values of θ, that is, $0 \le \theta < 0.2$ and $0.8 < \theta \le 1$, only the Frumkin adsorption isotherm is applicable to the adsorption of OPD H. Consequently, one can interpret that the Frumkin adsorption isotherm is more accurate, useful, and effective than the Temkin adsorption isotherm.

Standard Free Energy of Adsorption. The standard free energy of OPD H is given by the difference between the standard molar Gibbs free energy of OPD H and that of a number of water molecules on the adsorption sites of the electrode surface. Under the Frumkin adsorption conditions, the relation between the equilibrium constant (K) and the standard free energy (ΔG_θ^0) of OPD H is given as follows[33]

$$2.3RT \log K = -\Delta G_\theta^0 \qquad (8)$$

On Pt in 0.1 M KOH aqueous solution, using eqs 6 and 8, ΔG_θ^0 of OPD H is ($22.4 \ge \Delta G_\theta^0 \ge 16.5$) kJ·mol^{-1} for $K = 1.2 \cdot 10^{-4} \exp(2.4\theta)$ mol^{-1} and $0 \le \theta \le 1$. Similarly, on Ir in 0.1 M KOH aqueous solution, ΔG_θ^0 of OPD H is ($23.0 \ge \Delta G_\theta^0 \ge 17.1$) kJ·mol^{-1} for $K = 9.4 \cdot 10^{-5} \exp(2.4\theta)$ mol^{-1} and $0 \le \theta \le 1$. As stated above, these results imply an increase of ΔG_θ^0 of OPD H with θ ($0 \le \theta \le 1$). Note that ΔG_θ^0 is a negative number. The standard free energies (ΔG_θ^0) of OPD H and the equilibrium constants (K) for the Frumkin and Temkin adsorp-

Table 3. Comparison of the Standard Free Energies (ΔG_θ^0) of OPD H and the Equilibrium Constants (K) for the Frumkin and Temkin Adsorption Isotherms on Pt in 0.1 M KOH Aqueous Solution

adsorption isotherm	ΔG_θ^0 / kJ·mol^{-1}	K / mol^{-1}	θ
Frumkin[a]	$22.4 \geq \Delta G_\theta^0 \geq 16.5$	$1.2\cdot10^{-4} \leq K \leq 1.3\cdot10^{-3}$	$0 \leq \theta \leq 1$
Temkin[b]	$17.8 < \Delta G_\theta^0 < 21.0$	$7.7\cdot10^{-4} > K > 2.1\cdot10^{-4}$	$0.2 < \theta < 0.8$

[a] $K = 1.2\cdot10^{-4}\exp(2.4\theta)$ mol^{-1} (see Figure 8b). This result appears in ref 19 as unpublished data. [b] $K = 1.2\cdot10^{-3}\exp(-2.2\theta)$ mol^{-1} (see Figure 10b). Note that the Temkin adsorption isotherm is only valid and effective at $0.2 < \theta < 0.8$.

Table 4. Comparison of the Standard Free Energies (ΔG_θ^0) of OPD H and the Equilibrium Constants (K) for the Frumkin and Temkin Adsorption Isotherms on Ir in 0.1 M KOH Aqueous Solution

adsorption isotherm	ΔG_θ^0 / kJ·mol^{-1}	K / mol^{-1}	θ
Frumkin[a]	$23.0 \geq \Delta G_\theta^0 \geq 17.1$	$9.4\cdot10^{-5} \leq K \leq 1.0\cdot10^{-3}$	$0 \leq \theta \leq 1$
Temkin[b]	$18.3 < \Delta G_\theta^0 < 21.7$	$6.1\cdot10^{-4} > K > 1.6\cdot10^{-4}$	$0.2 < \theta < 0.8$

[a] $K = 9.4\cdot10^{-5}\exp(2.4\theta)$ mol^{-1} (see Figure 9b). This result appears in ref 19 as unpublished data. [b] $K = 9.4\cdot10^{-4}\exp(-2.2\theta)$ mol^{-1} (see Figure 11b). Note that the Temkin adsorption isotherm is only valid and effective at $0.2 < \theta < 0.8$.

tion isotherms on Pt and Ir in 0.1 M KOH aqueous solution are summarized in Tables 3 and 4, respectively.

Conclusions

On Pt and Ir in 0.1 M KOH aqueous solution, the Frumkin and Temkin adsorption isotherms (θ vs E), equilibrium constants [$K = 1.2\cdot10^{-4}\exp(2.4\theta)$ mol^{-1} for the Frumkin and $K = 1.2\cdot10^{-3}\exp(-2.2\theta)$ mol^{-1} for the Temkin adsorption isotherms on Pt and $K = 9.4\cdot10^{-5}\exp(2.4\theta)$ mol^{-1} for the Frumkin and $K = 9.4\cdot10^{-4}\exp(-2.2\theta)$ mol^{-1} for the Temkin adsorption isotherms on Ir], interaction parameters ($g = -2.4$ for the Frumkin and $g = 2.2$ for the Temkin adsorption isotherms on Pt and Ir), rates of change of the standard free energies ($r = -6.0$ kJ·mol^{-1} for $g = -2.4$ and $r = 5.5$ kJ·mol^{-1} for $g = 2.2$ on Pt and Ir) of OPD H with θ, and standard free energies [$(22.4 \geq \Delta G_\theta^0 \geq 16.5)$ kJ·mol^{-1} for $K = 1.2\cdot10^{-4}\exp(2.4\theta)$ mol^{-1} and $0 \leq \theta \leq 1$ and $(17.8 < \Delta G_\theta^0 < 21.0)$ kJ·mol^{-1} for $K = 1.2\cdot10^{-3}\exp(-2.2\theta)$ mol^{-1} and $0.2 < \theta < 0.8$ on Pt and $(23.0 \geq \Delta G_\theta^0 \geq 17.1)$ kJ·mol^{-1} for $K = 9.4\cdot10^{-5}\exp(2.4\theta)$ mol^{-1} and $0 \leq \theta \leq 1$ and $(18.3 < \Delta G_\theta^0 < 21.7)$ kJ·mol^{-1} for $K = 9.4\cdot10^{-4}\exp(-2.2\theta)$ mol^{-1} and $0.2 < \theta < 0.8$ on Ir] of OPD H are determined using the phase-shift method and correlation constants. The Frumkin adsorption isotherm is more accurate, useful, and effective than the Temkin adsorption isotherm.

At $0.2 < \theta < 0.8$, the two different adsorption isotherms, the Temkin and Frumkin or Langmuir adsorption isotherms, appear to fit the same data regardless of their adsorption conditions. The negative value ($g < 0$) of g for the Frumkin adsorption isotherms and the positive value ($g > 0$) of g for the Temkin adsorption isotherms are determined. A lateral attraction ($g < 0$) or repulsion ($g > 0$) interaction between the adsorbed OPD H species appears. The duality of the lateral attraction and repulsion interactions is probably a unique feature of OPD H on Pt, Ir, and Pt−Ir alloys in aqueous solutions.

The phase-shift method and correlation constants are probably the most accurate, useful, and effective ways to determine the Frumkin, Langmuir, and Temkin adsorption isotherms of OPD H and related electrode kinetic and thermodynamic parameters of the noble metals (alloys) in aqueous solutions.

Note Added after ASAP Publication: This paper was published on the Web on January 29, 2010. All instances of reversible hydrogen electrode (RHE) were changed to standard hydrogen electrode (SHE) in the text, graphics, and Supporting Information. The corrected version was reposted on June 16, 2010.

Supporting Information Available:

Comparisons of the experimentally determined Frumkin adsorption isotherm and three fitted Temkin adsorption isotherms (θ vs E) of OPD H on Pt and Ir in 0.5 M H_2SO_4 aqueous solution are shown in Supplementary Figures 1 and 2, respectively. This material is available free of charge via the Internet at http://pubs.acs.org.

Literature Cited

(1) Gileadi, E.; Kirowa-Eisner, E.; Penciner, J. *Interfacial electrochemistry*; Addison-Wesley: Reading, MA, 1975.
(2) Gileadi, E. *Electrode kinetics*; VCH: New York, 1993.
(3) Conway, B. E.; Jerkiewicz, G., Eds. *Electrochemistry and materials science of cathodic hydrogen absorption and adsorption; PV 94−21*; The Electrochemical Society: Pennington, NJ, 1995.
(4) Jerkiewicz, G.; Marcus, P., Eds. *Electrochemical surface science and hydrogen adsorption and absorption; PV 97−16*; The Electrochemical Society: Pennington, NJ, 1997.
(5) Jerkiewicz, G.; Feliu, J. M.; Popov, B. N., Eds. *Hydrogen at surface and interfaces; PV 2000−16*; The Electrochemical Society: Pennington, NJ, 2000.
(6) Gileadi, E. In *Electrosorption: Adsorption in electrochemistry*; Gileadi, E., Ed.; Plenum Press: New York, 1967; pp 1−18.
(7) Chun, J. H.; Ra, K. H. The phase-shift method for the Frumkin adsorption isotherms at the Pd/H_2SO_4 and KOH solution interfaces. *J. Electrochem. Soc.* **1998**, *145*, 3794–3798.
(8) Chun, J. H.; Ra, K. H.; Kim, N. Y. The Langmuir adsorption isotherms of electroadsorbed hydrogens for the cathodic hydrogen evolution reactions at the Pt(100)/H_2SO_4 and LiOH aqueous electrolyte interfaces. *Int. J. Hydrogen Energy* **2001**, *26*, 941–948.
(9) Chun, J. H.; Ra, K. H.; Kim, N. Y. Qualitative analysis of the Frumkin adsorption isotherm of the over-potentially deposited hydrogen at the poly-Ni/KOH aqueous electrolyte interface using the phase-shift method. *J. Electrochem. Soc.* **2002**, *149*, E325−330.
(10) Chun, J. H.; Ra, K. H.; Kim, N. Y. Langmuir adsorption isotherms of over-potentially deposited hydrogen at poly-Au and Rh/H_2SO_4 aqueous electrolyte interfaces: Qualitative analysis using the phase-shift method. *J. Electrochem. Soc.* **2003**, *150*, E207−217.
(11) Chun, J. H. Methods for estimating adsorption isotherms in electrochemical systems. U.S. Patent 6613218, 2003.
(12) Chun, J. H.; Jeon, S. K.; Kim, B. K.; Chun, J. Y. Determination of the Langmuir adsorption isotherms of under- and over-potentially deposited hydrogen for the cathodic H_2 evolution reaction at poly-Ir/aqueous electrolyte interfaces using the phase-shift method. *Int. J. Hydrogen Energy* **2005**, *30*, 247–259.
(13) Chun, J. H.; Jeon, S. K.; Ra, K. H.; Chun, J. Y. The phase-shift method for determining Langmuir adsorption isotherms of over-potentially deposited hydrogen for the cathodic H_2 evolution reaction at poly-Re/aqueous electrolyte interfaces. *Int. J. Hydrogen Energy* **2005**, *30*, 485–499.
(14) Chun, J. H.; Jeon, S. K.; Kim, N. Y.; Chun, J. Y. The phase-shift method for determining Langmuir and Temkin adsorption isotherms of over-potentially deposited hydrogen for the cathodic H_2 evolution reaction at the poly-Pt/H_2SO_4 aqueous electrolyte interface. *Int. J. Hydrogen Energy* **2005**, *30*, 1423–1436.
(15) Chun, J. H.; Kim, N. Y. The phase-shift method for determining adsorption isotherms of hydrogen in electrochemical systems. *Int. J. Hydrogen Energy* **2006**, *31*, 277–283.
(16) Chun, J. H.; Jeon, S. K.; Chun, J. Y. The phase-shift method and correlation constants for determining adsorption isotherms of hydrogen at a palladium electrode interface. *Int. J. Hydrogen Energy* **2007**, *32*, 1982–1990.
(17) Chun, J. H.; Kim, N. Y.; Chun, J. Y. Determination of adsorption isotherms of hydrogen and hydroxide at Pt-Ir alloy electrode interfaces using the phase-shift method and correlation constants. *Int. J. Hydrogen Energy* **2008**, *33*, 762–774.
(18) Chun, J. Y.; Chun, J. H. Correction and supplement to the determination of the optimum intermediate frequency for the phase-shift method [Chun et al Int. J. Hydrogen Energy 30 (2005) 247−259, 1423−1436]. *Int. J. Hydrogen Energy* **2008**, *33*, 4962–4965.
(19) Chun, J. Y.; Chun, J. H. A negative value of the interaction parameter for over-potentially deposited hydrogen at Pt, Ir, and Pt-Ir alloy electrode interfaces. *Electrochem. Commun.* **2009**, *11*, 744–747.
(20) Chun, J. Y.; Chun, J. H. Determination of adsorption isotherms of hydrogen on titanium in sulfuric acid solution using the phase-shift method and correlation constants. *J. Chem. Eng. Data* **2009**, *54*, 1236–1243.

(21) Chun, J. H.; Chun, J. Y. Determination of adsorption isotherms of hydrogen on zirconium in sulfuric acid solution using the phase-shift method and correlation constants. *J. Korean Electrochem. Soc.* **2009**, *12*, 26–33.

(22) Kvastek, K.; Horvat-Radosevic, V. Comment on: Langmuir adsorption isotherms of over-potentially deposited hydrogen at poly-Au and Rh/H_2SO_4 aqueous electrolyte interfaces; Qualitative analysis using the phase-shift method. *J. Electrochem. Soc.* **2003**, *150*, E207−217. *J. Electrochem. Soc.* **2004**, *151*, L9−10.

(23) Lasia, A. Comments on: The phase-shift method for determining Langmuir adsorption isotherms of over-potentially deposited hydrogen for the cathodic H_2 evolution reaction at poly-Re/aqueous electrolyte interfaces. *Int. J. Hydrogen Energy* **2005**, *30*, 485–499. *Int. J. Hydrogen Energy* **2005**, *30*, 913−917.

(24) Horvat-Radosevic, V.; Kvastek, K. Pitfalls of the phase-shift method for determining adsorption isotherms. *Electrochem. Commun.* **2009**, *11*, 1460–1463.

(25) Chun, J. H.; Ra, K. H.; Kim, N. Y. Response to comment on: Langmuir adsorption isotherms of over-potentially deposited hydrogen at poly-Au and Rh/H_2SO_4 aqueous electrolyte interfaces; Qualitative analysis using the phase-shift method. *J. Electrochem. Soc.* **2003**, *150*, E207. *J. Electrochem. Soc.* **2004**, *151*, L11−13.

(26) Chun, J. H.; Jeon, S. K.; Kim, N. Y.; Chun, J. Y. Response to comments on: The phase-shift method for determining Langmuir adsorption isotherms of over-potentially deposited hydrogen for the cathodic H_2 evolution reaction at poly-Re/aqueous electrolyte interfaces. *Int. J. Hydrogen Energy* **2005**, *30*, 485–499. *Int. J. Hydrogen Energy* **2005**, *30*, 919−928.

(27) In our e-mail communications, Horvat-Radosevic et al. admitted that all of their objections to the phase-shift method in ref 24 were confused and misunderstood. They still do not understand and accept the phase-shift method itself without reliable simulation or experimental data. .

(28) Gileadi, E.; Kirowa-Eisner, E.; Penciner, J. *Interfacial electrochemistry*; Addison-Wesley: Reading, MA, 1975; pp 6, 72−73.

(29) Gileadi, E.; Kirowa-Eisner, E.; Penciner, J. *Interfacial electrochemistry*; Addison-Wesley: Reading, MA, 1975; pp 86−93.

(30) Gileadi, E. *Electrode kinetics*; VCH: New York, 1993; pp 291−303.

(31) Harrington, D. A.; Conway, B. E. AC impedance of faradaic reactions involving electrosorbed intermediates-I. Kinetic theory. *Electrochim. Acta* **1987**, *32*, 1703–1712.

(32) Gileadi, E.; Kirowa-Eisner, E.; Penciner, J. *Interfacial electrochemistry*; Addison-Wesley: Reading, MA, 1975; pp 82−86.

(33) Gileadi, E. *Electrode kinetics*; VCH: New York, 1993; pp 261−280.

(34) Bockris, J. O'M.; Reddy, A. K. N.; Gamboa-Aldeco, M. *Modern electrochemistry*, 2nd ed.; Kluwer Academic/Plenum Press: New York, 2000; Vol. 2A, pp 1193−1197.

(35) Oxtoby, D. W.; Gillis, H. P.; Nachtrieb, N. H. *Principles of modern chemistry*, 5th ed.; Thomson Learning Inc.: New York, 2002; p 446.

(36) Gileadi, E. *Electrode kinetics*; VCH: New York, 1993; pp 303−305.

Received for review October 6, 2009. Accepted January 15, 2010. This work was supported by the Research Grant of Kwangwoon University in 2009.

JE900805Q